Received: 28 June 2023 | Revised: 30 July 2023 | Accepted: 23 August 2023

DOI: 10.1002/pamm.202300063

RESEARCH ARTICLE

Dimensional reduction for parametric projection-based reduced-order models in crash

Mathias Lesjak[1,2] | **Fabian Duddeck**[2]

[1]BMW Group, Research and Innovation Center, Munich, Germany

[2]Technical University of Munich, TUM School of Engineering and Design, Munich, Germany

Correspondence
Mathias Lesjak, BMW Group, Research and Innovation Center, Munich, Germany.
Email: mathias.lesjak@bmw.de

Abstract

Modern car development regarding passive safety strongly relies on finite element simulations. Many simulations are required to assess the behavior of the design regarding minor parameter variations that occur naturally in hardware tests. This avoids costly revisions later in the design process when the first hardware tests are conducted. However, due to the immense computational costs, multiquery analyses such as robustness studies, optimization, and uncertainty quantification are currently not feasible for large simulation models. Reduced-order modeling uses already generated data to accelerate future simulations. Using a data-driven method, a low-rank structure can be identified. The generated mapping subsequently expresses the governing equations regarding the reduced variables. Projection-based model order reduction (MOR) is therefore physics-based and has no black-box character as classical machine learning models. The accuracy of the reduced-order model (ROM) heavily relies on the dimensional reduction. Currently, proper orthogonal decompositionis most commonly used. However, this linear method is variance-based and nonlinear correlation cannot be resolved requiring more dimensions in the approximation. Effective hyperreduction depends on the dimension of the ROM. Hence, we provide an overview of different strategies for parametric MOR in the context of highly nonlinear solid dynamics, discussing potential benefits and drawbacks. We show a successful application of the local reduced-order bases approach to a crash problem and present first results of an autoencoder that is a nonlinear-dimensional reduction.

1 | INTRODUCTION

While virtual development using the finite element method (FEM) idealizes the model, hardware crash tests contain numerous uncertainties, especially in the early design phase. These reach from differences in the hardware to deviations in the test conditions. Engineers are therefore also interested in how the system response changes when varying the input parameters; otherwise, the probability of failing the final examination is high. Methods investigating the system response around a parameter point usually require numerous system evaluations that is currently infeasible for large models due to

the long simulation times. Model order reduction (MOR) reduces the computational effort and therefore the simulation time by using previous knowledge about the model. According to [1], MOR can be categorized into three different types: data-fit models, projection-based models, and hierarchical models. Data-fit models are purely data-driven models that learn correlations in the data, usually blind to the underlying physics. Gaussian process regression is a popular technique in this field [2, 3]. Hierarchical models are physics-based models that rely on additional simplifications. These can be physical and mathematical assumptions resulting in the application of linear theories, the use of coarser grids, or looser residual tolerances. Fehr et al. [4], for example, reduced a gokart frame by dividing it into linear and nonlinear parts.

In this work, we focus on projection-based MOR. pROMs were first introduced in the field of turbulent flows [5] where a low-rank structure was assumed in the flow field. Later, projection-based MOR was transferred to other disciplines such as control and solid dynamics. MOR is usually separated into an offline phase and an online phase. The offline phase is associated with the construction of the ROM and the online phase with the ROM evaluation. The first part of the offline phase is the dimensional reduction. The (truncated) proper orthogonal decomposition (POD) is the most commonly used linear reduction method that creates a low-dimensional subspace based on the training data. Afterward, the solution of the high-dimensional model (HDM) is restricted to lie in this subspace whereby a residual is formed. Depending on the treatment of the residual, different pROMs can be formed. The interested reader is referred to Carlberg et al. [6] for a discussion of residual minimization.

To achieve speedup, nonlinear models require an additional approximation layer termed hyperreduction. Hyperreduction approximates the nonlinear term, which otherwise still scales with the dimension of the HDM. Only if the nonlinearity is of a particular type, for instance, of polynomial order [7, 8], a precomputation of the nonlinear operator in reduced space is possible that makes hyperreduction unnecessary. However, systems in crash are not of this type and hyperreduction is required. While different methods for hyperreduction exist, for example, the empirical interpolation method (EIM) [9] and its discrete counterpart DEIM [10], energy-conserving sampling and weighting (ECSW), as proposed by Farhat et al. [11], is the most popular method in solid dynamics. This is due to preservation of the Lagrangian structure of the problem and the resulting stability properties [12].

To summarize, the speedup in crash models can be achieved by basically two mechanisms: hyperreduction and a probably larger timestep in the explicit time integration [11, 13]. So far, pROMs in crash were mainly applied to reproductive examples [14]; however, the key to use them in the previously mentioned multiquery analyses is the variation of the input parameters. Therefore, parametric pROMs are the subject of this publication. The key question is how to properly create a parametric pROM, and more specifically, how to effectively reduce the dimension of the problem as the global POD approach reaches its limits [3]. One approach for parametric MOR is manifold interpolation [15], however, only suitable for linear models. The local reduced-order bases (lROB) approach [16] divides the set of training data first into subsets using a clustering algorithm. These subsets, also named clusters, divide the state space into subregions, for each of which an ROB is computed. In the online phase, as the solution evolves in time, the most suitable ROB is chosen. The lROB method is easily extensible to ECSW [17], although special attention must be paid to problems including path-dependent materials. Autoencoder (AE) is a global nonlinear approach and has recently been used by [18, 19]. In the AE ROM, the reduced basis is replaced by the Jacobian matrix of the AE. Also, ECSW can be extended to be compatible with nonlinear dimension reduction models [20]. Another unanswered question for models involving shell formulations is the treatment of the different types of variables. As mentioned by Farhat et al. [11], displacements and rotations have different variable characteristics. Bach [14] treated displacements and rotations separately; however, no investigation has been carried out if a combined treatment is preferable.

2 | METHODOLOGY

2.1 | Governing equations

We first introduce the governing equations arising from the FEM when applied to the underlying equations of motion:

$$\mathbf{M}(\mu)\ddot{x} + f_{int}(t, x, \dot{x}, \mu) = f_{ext}(t, x, \mu), \tag{1}$$

where $\mathbf{M} \in \mathbb{R}^{n\times n}$ is the mass matrix, $x \in \mathbb{R}^n$ is the high-dimensional state vector, n is the number of degrees of freedom (DoF) in the system, $\dot{x} = \frac{\mathrm{d}x}{\mathrm{d}t}$ is the derivative of x with respect to time t, $f_{int} \in \mathbb{R}^n$ and $f_{ext} \in \mathbb{R}^n$ are the internal and external force vector, respectively, and $\mu \in \mathbb{R}^p$ is the parameter vector containing the p varied parameters. Typical car

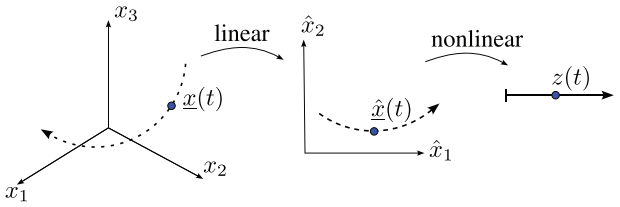

FIGURE 1 One-dimensional manifold embedded in three-dimensional space.

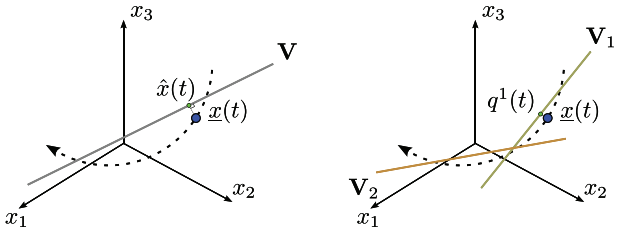

FIGURE 2 Global ROB approach (on the left side) versus local ROB approach (on the right side).

structures are thin-walled and described by shell formulations in the FEM models. Therefore, x contains translatory and rotatory DoF. In addition to Equation (1), we consider the variational form thereof, as it will be useful for the derivation of the AE ROM. It reads:

$$\delta v_i(\mathbf{M}^{ij}\ddot{x}_j + f^i_{int} - f^i_{ext}) = 0, \tag{2}$$

where $\delta v(x) = \delta v_i N^i(x)$ is a continuous test function fulfilling the boundary conditions, and summation of pairwise appearing indices is implied. The trial function has the same shape functions $N^i(x)$ as the test function and is given as $x(t,x) = x_i(t)N^i(x)$. The scalar values δv_i are often termed virtual nodal velocities, Equation (2) can be considered as power balance, and therefore, it is also known as the principle of virtual power. Since δv_i can be chosen arbitrarily, Equation (2) is equivalent to Equation (1).

2.2 | Model order reduction

We begin to motivate MOR by its underlying assumption that the solution of a high-dimensional system lies on a low-dimensional manifold. Figure 1 shows an one-dimensional curved manifold embedded in a three-dimensional space. Assuming that this line lies in a plane, it can be reduced to two dimensions using a linear dimensionality reduction. However, nonlinear data require a nonlinear dimensionality reduction to fully reduce the manifold to its intrinsic dimension, which is one for this line. It is important to emphasize that we are considering dimensionality reduction without approximation error in this illustrative example.

In contrast, Figure 2 shows linear dimensionality reduction to one dimension with precision loss, as a linear reduction is not able to approximate this nonlinear data. On the left side of Figure 2, the global linear approach is depicted. To avoid large errors, more dimensions must be retained. In contrast, on the right side, the lROB approach is depicted. The manifold is divided into multiple subregions, of which each is approximated by a linear subspace $\mathbf{V}_i$. Thereby, the dimension can be chosen low, ensuring accuracy and enabling hyperreduction.

Next, we discuss how linear and nonlinear dimensional reduction is used to formulate the ROMs. They are stated without further derivation as this would go beyond the scope of this work and is known in the literature. We begin with POD, which is a linear method. The high-dimensional state vector x is represented as a linear superposition of deformation modes, which are the columns of the ROB $\mathbf{V} \in \mathbb{R}^{n\times k}$, and the reduced amplitudes stored in the reduced state vector $\hat{x} \in \mathbb{R}^k$ with $k \ll n$:

$$x(t) \approx \tilde{x}(t) = \mathbf{V}\hat{x}(t), \tag{3}$$

where $\tilde{x} \in \mathbb{R}^n$ is the reconstructed state. Next, Equation (3) is inserted into Equation (1). The resulting residual is enforced to be orthogonal to the ROB $\mathbf{V}$ and we obtain the global linear ROM:

$$\underbrace{\mathbf{V}^T\mathbf{M}\mathbf{V}}_{\tilde{\mathbf{M}}}\ddot{\hat{x}} + \mathbf{V}^T(f_{int}(\mathbf{V}\hat{x}, \mathbf{V}\dot{\hat{x}}, \mu) - f_{ext}(t, \mathbf{V}\hat{x}, \mu)) = 0. \tag{4}$$

Now, we transfer Equation (4) to the lROB case by considering a discrete timestep $t = t_n$ and allowing the ROB $\mathbf{V_n}$ to depend on the current state $x(t_n) = x_n$.

$$\mathbf{V}_n^T\mathbf{M}\mathbf{V}_n\ddot{\tilde{x}}_n^{k_n} + \mathbf{V}_n^T(f_{int}(\tilde{x}_n, \dot{\tilde{x}}_n, \mu) - f_{ext}(t_n, \tilde{x}_n, \mu)) = 0, \tag{5}$$

where $\ddot{\tilde{x}}_n^{k_n}$ is the reduced acceleration at time t_n of cluster dimension k_n and $\tilde{x}$ is the reconstructed state, which can be calculated as the sum over all cluster states $q_n^r \in \mathbb{R}^{k_n}$ at time t_n multiplied with the corresponding reduced basis $\mathbf{V_n} \in \mathbb{R}^{n \times k_n}$:

$$\tilde{x}_n = x_0 + \sum_{m=1}^{n_c} \mathbf{V}_r q_n^m, \tag{6}$$

where n_c is the number of clusters. When solving Equation (5), additional steps are required. At each time step, it has to be checked whether a change in the subdomain is necessary. This involves computing the distance of the current state to all cluster centers. If the distance to a cluster other than the one currently used is smaller, a cluster change is necessary. The distance calculation has to be formulated in reduced dimensions as well. Otherwise, the computation of the norm would scale with the HDM dimension, and no speedup can be achieved. However, the theory is beyond the scope of this work and we refer to Amsallem et al. [16] for the complete theory. Finally, we introduce the ROM based on nonlinear dimensionality reduction. A nonlinear function Γ maps a low-dimensional variable $z \in \mathbb{R}^r$ with dimension r to a higher-dimensional state $\hat{x} \in \mathbb{R}^k$:

$$\hat{x}(t) \approx \tilde{\hat{x}}(t) = \Gamma(z(t)). \tag{7}$$

To insert Equation (7) into Equation (4), we have to differentiate it twice with respect to time. Applying the chain rule yields:

$$\dot{\hat{x}} = \frac{\partial \Gamma}{\partial z}\dot{z}, \tag{8}$$

$$\ddot{\hat{x}} = \frac{\partial \Gamma}{\partial z}\ddot{z} + \frac{\partial^2 \Gamma}{\partial z^2}\dot{z}\dot{z}, \tag{9}$$

where $\mathbf{J} = \frac{\partial \Gamma}{\partial z} \in \mathbb{R}^{k \times r}$ is the Jacobian of the AE and $\mathbf{H} = \frac{\partial^2 \Gamma}{\partial z^2} \in \mathbb{R}^{k \times r \times r}$ its Hessian. Next, according to the principle of virtual power, we have to adjust the test function describing the admissible velocities. The velocities live in the tangent space to the manifold that is prescribed by the columns of the Jacobian $\mathbf{J}$. Combining the linear global ROMs admissible velocities with the AE yields:

$$\delta v_i = V_{ij} J(z)^{jk} \delta \dot{z}_k. \tag{10}$$

Putting all the equations together and considering that the virtual latent velocities $\dot{z}_k$ are arbitrary, we obtain the final ROM:

$$\mathbf{J}^T\tilde{\mathbf{M}}\mathbf{J}\ddot{z} + \mathbf{J}^T\tilde{\mathbf{M}}\mathbf{H}\dot{z}\dot{z} + \mathbf{J}^T\mathbf{V}^T(f_{int}(\mathbf{V}\Gamma(z), \mathbf{V}\mathbf{J}\dot{z}, \mu) - f_{ext}(t, \mathbf{V}\Gamma(z), \mu)) = 0. \tag{11}$$

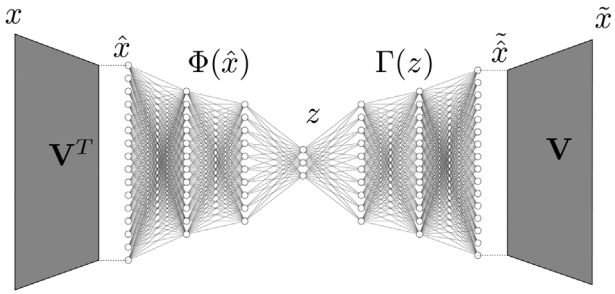

FIGURE 3 AE-based pROM using a linear outer layer and an AE to resolve the nonlinear correlations.

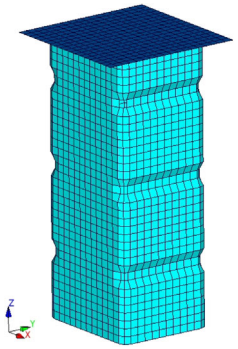

FIGURE 4 Crash box model in undeformed configuration.

The introduced ROMs are continuous in time and are integrated using the central difference method:

$$\ddot{x}|_{t=t_n} = \ddot{x}^n \approx \frac{\dot{x}^{n+\frac{1}{2}} - \dot{x}^{n-\frac{1}{2}}}{\Delta t}, \tag{12}$$

$$\dot{x}|_{t=t_n+\frac{1}{2}} = \dot{x}^{n+\frac{1}{2}} \approx \frac{x^{n+1} - x^n}{\Delta t}, \tag{13}$$

$$\Rightarrow \ddot{x}^n \approx \frac{x^{n+1} - 2x^n + x^{n-1}}{\Delta t^2}. \tag{14}$$

In addition, the unknown latent velocity $\dot{z}_n$ in the nonlinear term of Equation (11) at time t_n is approximated by the previous velocity $\dot{z}_{n-1/2}$ at the half-time step to ensure an explicit scheme. The AE ROM equation (11) is illustrated in Figure 3. First, the dimension is reduced using POD. Afterward, the nonlinear correlations are resolved using an AE.

3 | RESULTS

3.1 | Crash model

We use the crash box model as seen in Figure 4. The crash box is modeled by 1864 fully integrated shell elements and is impacted by a rigid plate. The model is a slightly adapted version of the crash box model at dynaexamples.com and will be sent on request. For the parametric setting, the thickness of the tube and the mass of the rigid plate are varied between and 2.5 mm and and 162 kg, respectively. A total of 30 samples are drawn using Latin Hypercube sampling, of which 27 are used for training and 3 are used to test the framework. The distribution of parameter points can be seen in Figure 5. The test points are chosen to represent a crash box with high and with low deformation. In the following,

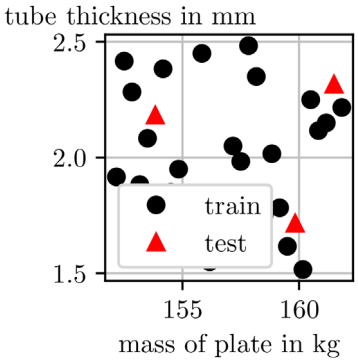

FIGURE 5 Sampling points in parameter space.

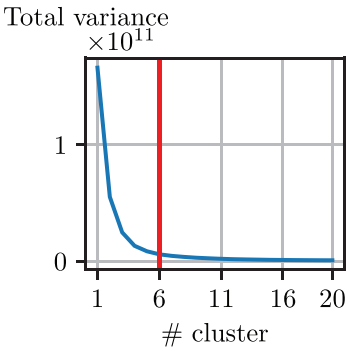

FIGURE 6 Total variance of the k-means clustering for a different number of clusters.

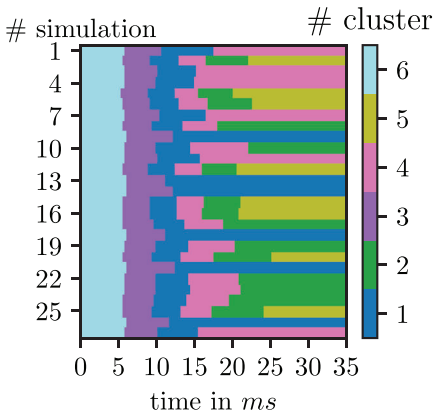

FIGURE 7 Assignment of snapshots to the clusters.

only the highly deforming test case is considered as experience has shown that it is the critical one. For the dimensional reduction, snapshots are taken every 1.5 ms for each simulation of length 35 ms resulting in 94 527 snapshots of dimension $n = 11\,544$.

3.2 | Dimensionality reduction

Except for the reduced dimension, there are no hyperparameters in the global ROM. In contrast, with the lROB ROM, the number of clusters must be selected first. We use the elbow method to choose a reasonable number of clusters by observing the total variance of the k-means clustering. Figure 6 shows the total variance for different cluster numbers. We select six clusters to construct the ROM. The clustering results are shown in Figure 7, where each row corresponds to a

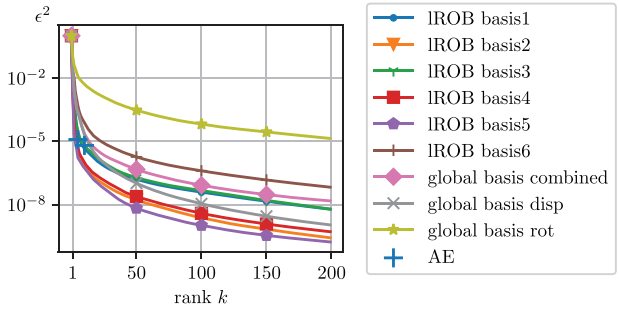

FIGURE 8 Approximation error of the dimensionality reduction.

training simulation of length 35 ms and each color corresponds to a cluster. K-means clustering is based on L^2 distances and the solution vector is the displacement vector. Therefore, a partition of the solution along the simulation time can be observed.

Finally, the offline accuracy, which is the pure approximation quality of the dimensionality reduction, is assessed. The error is defined as:

$$\epsilon^2 = \frac{\|\mathbf{U} - \tilde{\mathbf{U}}\|_{\mathrm{F}}^2}{\|\mathbf{U}\|_{\mathrm{F}}^2} \tag{15}$$

with the snapshot matrix $\mathbf{U} \in \mathbb{R}^{n \times n_{\mathrm{snaps}}}$, its approximation $\tilde{\mathbf{U}}$, the Frobenius norm $\|\|_{\mathrm{F}}$, and the number of snapshots in the cluster n_{snaps}. Figure 8 shows the error for increasing approximation ranks k for the global reduced basis and the local reduced bases. First, a combined reduction is preferable as the added error to the displacements is still lower than the approximation error of the rotations alone. Therefore, the depicted lROB error is regarding a combined treatment. Second, except for basis 6, all local bases approximate the data better than the global basis. Basis 6 corresponds to the cluster containing snapshots from the first approximately 6 ms, as can be seen in Figure 7. The AE can further reduce the global data to 5 and 10 dimension maintaining a higher accuracy than the global linear basis.

3.3 | ROM accuracy

Next, the ROMs are created using the results from the offline phase, and their accuracy is assessed. Only displacement DoFs are considered for the online error calculation, as they are usually important for crash applications. We define the online error as:

$$\epsilon = \frac{\langle \|u(t) - \tilde{u}(t)\|_2^2 \rangle^{\frac{1}{2}}}{\langle \|u(t)\|_2^2 \rangle^{\frac{1}{2}}}, \tag{16}$$

where $\langle \cdot \rangle$ is the temporal averaging operator defined as:

$$\langle u(t) \rangle = \sum_{i=1}^{n} \frac{u(t_i)}{n}, \tag{17}$$

and $u(t)$ and $\tilde{u}(t)$ are the FOM and ROM solution, respectively. In Figure 9, the error ϵ can be seen for different types of ROMs for different dimension k. First, the result of the offline phase can be found here as well, that is, a combined treatment of rotations and displacements is preferable. For $k = 60$, the combined ROM is as accurate as the ROM with 60 dimensions for the rotations solely. It can be seen that the displacement ROM converges faster to small errors than the rotation ROM. For higher ranks, the leading error sources are the rotations, as the error of the rotation ROM and the combined ROM overlap. Second, the lROB ROM converges faster to smaller errors than the global ROMs. This mirrors

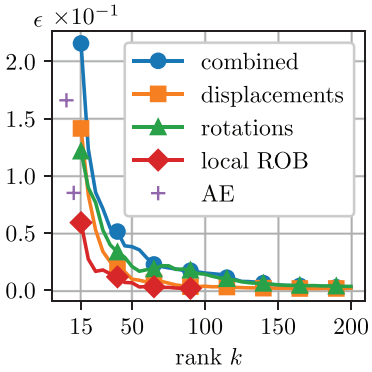

FIGURE 9 ROM accuracy.

the better approximation quality of the local bases shown in Figure 7. Third, the AE ROM outperforms the global ROMs for 10 dimensions. Also, the AE ROM with five dimensions has a lower error than the combined ROM for $k = 15$.

4 | CONCLUSION

In this work, three different types of dimensionality reduction are discussed, namely, globally linear, locally linear, and globally nonlinear. The methods are chosen for their suitability for crash problems, which implies compatibility with hyperreduction. While the focus of this work is not computational speedup, it is the approximation quality of dimensionality reduction and the associated accuracy of the ROM for parametric problems in crash. An accurate mapping to a low dimension enables hyperreduction, which will lead to speedup. We show that a combined treatment of rotations and displacements yields an accurate mapping and mitigates the influence of the hard-to-reduce rotations. However, the global ROM requires many dimensions to accurately predict the systems evolution making hyperreduction impractical. The lROB ROM yields higher accuracy using less dimensions. Hyperreduction benefits directly, as the dimension of the reduced basis directly influences size of the associated optimization problem. In addition, the optimization problem is split into one even smaller problem for each cluster. The lROB ROM preserves linear properties such as a monotonic decrease in error with increasing dimensions. Finally, the AE can resolve further nonlinear correlations. However, compared to the lROB approach, it is more sophisticated and still in an early research stage with many unanswered research questions. To conclude, the lROB approach is currently most promising and the best compromise between complexity and accuracy for highly nonlinear parametric problems.

ACKNOWLEDGMENTS

Open access funding enabled and organized by Projekt DEAL.

ORCID

Mathias Lesjak https://orcid.org/0000-0001-6027-7851

REFERENCES

1. Eldred, M., & Dunlavy, D. (2006). Formulations for surrogate-based optimization with data fit, multifidelity, and reduced-order models. In *11th AIAA/ISSMO Multidisciplinary Analysis and Optimization Conference*.
2. Guo, M., & Hesthaven, J. S. (2018). Reduced order modeling for nonlinear structural analysis using Gaussian process regression. *Computer Methods in Applied Mechanics and Engineering*, *341*, 807–828.
3. Czech, C., Lesjak, M., Bach, C., & Duddeck, F. (2022). Data-driven models for crashworthiness optimisation: Intrusive and non-intrusive model order reduction techniques. *Structural and Multidisciplinary Optimization*, *65*, 190.
4. Fehr, J., Holzwarth, P., & Eberhard, P. (2016). Interface and model reduction for efficient explicit simulations - A case study with nonlinear vehicle crash models. *Mathematical and Computer Modelling of Dynamical Systems*, *22*, 380–396.
5. Sirovich, L. (1987). Turbulence and the dynamics of coherent structures. III. Dynamics and scaling. *Quarterly of Applied Mathematics*, *45*, 583–590.
6. Carlberg, K., Barone, M., & Antil, H. (2017). Galerkin v. least-squares Petrov-Galerkin projection in nonlinear model reduction. *Journal of Computational Physics*, *330*, 693–734.

7. Rowley, C. W., Colonius, T., & Murray, R. M. (2004). Model reduction for compressible flows using pod and Galerkin projection. *Physica D: Nonlinear Phenomena*, *189*, 115–129.
8. Barbič, J., & James, C. W. (2005). Real-time subspace integration for st. Venant-Kirchhoff deformable models. *Acm Transactions on Graphics*, *24*, 982–990.
9. Barrault, M., Maday, Y., Nguyen, N. C., & Patera, A. T. (2004). An 'Empirical Interpolation' method: Application to efficient reduced-basis discretization of partial differential equations. *Comptes Rendus Mathematique*, *339*, 667–672.
10. Chaturantabut, S., & Sorensen, D. C. (2010). Nonlinear model reduction via discrete empirical interpolation. *SIAM Journal on Scientific Computing*, *32*, 2737–2764.
11. Farhat, C., Avery, P., Chapman, T., & Cortial, J. (2014). Dimensional reduction of nonlinear finite element dynamic models with finite rotations and energy-based mesh sampling and weighting for computational efficiency. *International Journal for Numerical*, *98*, 625–662.
12. Farhat, C., Chapman, T., & Avery, P. (2015). Structure-preserving, stability, and accuracy properties of the energy-conserving sampling and weighting method for the hyper reduction of nonlinear finite element dynamic models. *International Journal for Numerical*, *102*, 1077–1110.
13. Bach, C., Song, L., Erahrt, T., & Duddeck, F. (2018). Stability conditions for the explicit integration of projection based nonlinear reduced-order and hyper reduced structural mechanics finite element models. arXiv preprint arXiv:1806.11404.
14. Bach, C., Ceglia, D., Song, L., & Duddeck, F. (2019). Randomized low-rank approximation methods for projection-based model order reduction of large nonlinear dynamical problems. *International Journal for Numerical*, *118*, 209–241.
15. Amsallem, D., Cortial, J., Carlberg, K., & Farhat, C. (2009). A method for interpolating on manifolds structural dynamics reduced-order models. *International Journal for Numerical Methods in Engineering*, *80*, 1241–1258.
16. Amsallem, D., Zahr, M. J., & Farhat, C. (2012). Nonlinear model order reduction based on local reduced-order bases. *International Journal for Numerical*, *92*, 891–916.
17. Grimberg, S., Farhat, C., Tezaur, R., & Bou-Mosleh, C. (2021). Mesh sampling and weighting for the hyperreduction of nonlinear Petrov-Galerkin reduced-order models with local reduced-order bases. *International Journal for Numerical*, *122*, 1846–1874.
18. Fulton, L., Modi, V., Duvenaud, D., Levin, D. I. W., & Jacobson, A. (2019). Latent-space dynamics for reduced deformable simulation. *Computer Graphics Forum*, *38*, 379–391.
19. Shen, S., Shao, T., Zhou, K., Jiang, C., Luo, F., & Yang, Y. (2022). Hod-net: High-order differentiable deep neural networks and applications. In *Proceedings of the AAAI Conference on Artificial Intelligence*, Vol. *36*.
20. Jain, S., & Tiso, P. (2019). Hyper-reduction over nonlinear manifolds for large nonlinear mechanical systems. *Journal of Computational and Nonlinear Dynamics*, *14*(8).

How to cite this article: Lesjak, M., & Duddeck, F. (2023). Dimensional reduction for parametric projection-based reduced-order models in crash. *Proceedings in Applied Mathematics and Mechanics*, *23,* e202300063. https://doi.org/10.1002/pamm.202300063